Digital Object Identifier 10.1109/IECON48115.2021.9589995

IECON 2021 – 47th Annual Conference of the IEEE Industrial Electronics Society

# Stability Enhancement for Single-Loop Voltage Controlled Voltage-Source Converters with LC-Filter

Ziqi Zhou
Sante Pugliese
Marco Liserre

## Suggested Citation

Z. Zhou, S. Pugliese and M. Liserre, "Stability Enhancement for Single-Loop Voltage Controlled Voltage-Source Converters with LC-Filter," IECON 2021 – 47th Annual Conference of the IEEE Industrial Electronics Society, 2021.

# Stability Enhancement for Single-Loop Voltage Controlled Voltage-Source Converters with LC-Filter

Ziqi Zhou, Sante Pugliese, and Marco Liserre
*Chair of Power Electronics*
*Kiel University*
Kiel, Germany
{ziqi, sapu, ml}@tf.uni-kiel.de

***Abstract*—Voltage controlled voltage source converters (VSCs) have been widely applied in microgrids, uninterruptible power sources, smart transformer and 400 Hz ground power units for airplanes, etc. An LC filter is generally adopted to attenuate high frequency switching harmonic and to improve the qualities of output voltage and current for grid or loads. Nevertheless, VSCs have to trade-off between the stability characteristic and the ability of switching harmonics suppression when a single-loop voltage control method is adopted. In general, the resonant frequency $\omega_r$ of LC filter should be less than 1/4 of sampling frequency $\omega_s$ to ensure sufficient attenuation of the switching harmonic. However, $\omega_r$ should be higher than 1/3 of $\omega_s$ for the system stability when a proportional-resonant (PR) controller with a positive proportional gain is implemented. This paper proposes a feedback of modulation voltage (FMV) control design method for single-loop control to ensure stability condition in a higher frequency range and good switching harmonics suppression at the same time. Finally, simulation results are provided to verify the effectiveness of the proposed method.**

***Index Terms*—Feedback of modulation voltage, low *LC*-resonant-frequency, negative proportional gain, single-loop control, stability design, voltage-source converter.**

## I. INTRODUCTION

Voltage-controller voltage source inverter (VSIs) are increasingly applied in distributed power generation system [1], 400-Hz ground power units for airplane [2], uninterruptible power supplies [3] and smart transformer [10]. Generally, VSIs interact with the grid through LC-filters to attenuate high frequency switching harmonics to improve quality of output voltage and current waveforms. However, the resonance brought by LC filters will significantly challenge the stability characteristic of VSIs [4].

For damping the resonance and to enhance system robustness, many control strategies have been proposed and can be classified into two groups, i.e. passive damping method [5] and active method [6]. Passive damping methods suppress the resonance peak by paralleling or connecting a resistor with the inductor or capacitor of the LC filter. The method is effective but adds extra power loss. Active damping generally utilizes an additional feedback loop of system state-variables in the control system to emulate the passive damping method, thus the power loss can be avoided. This method is also called double-loop control method. However, the double-loop control method requires additional current sensors and hardly meet the stability requirements for low pulse-ratio inverters, e.g. a 400-Hz ground power units [2]. Therefore, a single-loop voltage control is much more suitable for low-ratio inverters [7].

On the basis, many papers have investigated the stability characteristic of the single-loop method and developed many control strategies to improve the stability performance and dynamic response. It's revealed that the control system with a single-loop method can stabilize itself when resonant frequency $f_r$ is above $f_s/3$ ($f_s$ is the sampling frequency) with digital delay [4], [8]. In [2], a resonant (R) controller instead of a proportional-resonant (PR) controller is adopted to regulate the capacitor voltage. The analysis shows that the stable region can be extended to $f_r > f_s/6$. In [9], a negative proportional gain $k_p$ is applied for PR controller, and the system can be stable when $f_r$ is less than $f_s/3$.

Then, an improved single-loop control scheme with the feedback of modulation voltage is proposed in this paper to ensure stability when the resonant frequency is less than $f_s/4$. In this method, the modulation voltage is delayed of one sampling step and is fed back to the control system with a proportional gain $k_{FMV}$ on the basis of traditional single-loop control. The analysis shows that the stable region of the system will be affected by the values of the proportional gain $k_{FMV}$. In further, a control design method is proposed to extend the stable region to $(0, f_s/2)$ at most. Simulation results are provided to validate the correctness of the theoretical analysis.

Following the introduction, Section II analyzes the stable region of the conventional single-loop based control system. In Section III, feedback of modulation voltage (FMV) control method is proposed and the stable region of the control system with FMV method is analyzed. Section IV show simulation results to verify the effectiveness and correctness of the FMV method. Finally, Section V finally concludes the paper.

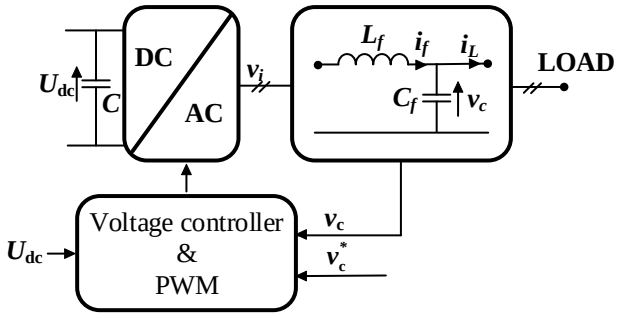


Fig. 1. A single-phase voltage-controlled VSC with single-voltage-loop control.

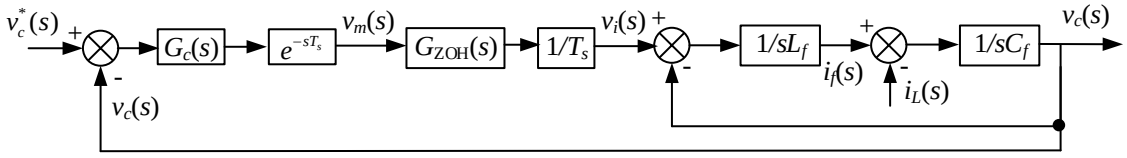


(a)

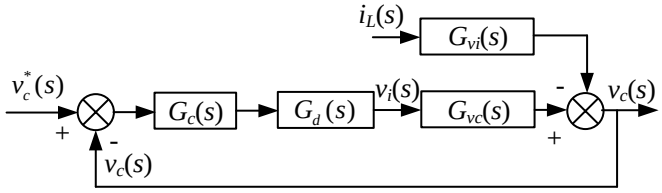


(b)

Fig. 2. Single-loop voltage control diagram in the continuous *s*-domain. (a) Block diagram. (b) Equivalent diagram.

## II. Conventional Stability Design for Single-Voltage-Loop Control Method

Fig. 1 shows a control scheme of a single-phase voltage source inverter for simplicity of analysis, where the conventional single-loop voltage control is implemented instead of the conventional double-loop control. $L_f$ and $C_f$ represents the filter inductor and the filter capacitor of LC filter, respectively. $C$ represents the capacitor of DC source. $i_f$ indicates filter inductor current, $i_L$ indicates load current, $U_{dc}$ represents the voltage of DC bus. $v_c$ indicates filter capacitor voltage. Fig. 2(a) shows the corresponding voltage control diagram in the continuous *s*-domain where $G_c(s)$ is the PR controller, given as

$$G_c(s) = k_p + \frac{k_r \omega_b s}{s^2 + 2\omega_b s + \omega_o^2}, \omega_o = 2\pi f_o, \tag{1}$$

where $k_p$ is the proportional gain and $k_r$ is the resonant gain. $\omega_o$ is the fundamental angular frequency. As fundamental frequency $\omega_o$ is far less than resonant frequency $\omega_r$, $G_c(z)$ can be approximated to proportional gain $k_p$ when analyzing system stability caused by the high-frequency filter resonance.

$G_{ZOH}(s)$ is the equivalent half sampling period of zero-order-hold (ZOH) delay, $e^{-sT_s}$ represents one sampling period of computation delay. $v_m(s)$ represents the modulation voltage, $v_i(s)$ represents the inverter side output voltage and $v_c^*(s)$ represents the reference voltage. The equivalent diagram is shown in Fig. 2(b). In the figure, $G_d(s)$ is the combination of $G_{ZOH}(s)$ and $e^{-sT_s}$. $G_{vc}(s)$ and $G_{vi}(s)$ are the transfer functions from converter-side voltage $v_i(s)$ to capacitor voltage $v_c(s)$ and from load current $i_L(s)$ to capacitor voltage $v_c(s)$ respectively, expressed as

$$\begin{cases} G_{vc}(s) = \dfrac{v_c(s)}{v_i(s)} = \dfrac{\omega_r^2}{s^2 + \omega_r^2} \\ G_{vi}(s) = \dfrac{v_c(s)}{i_L(s)} = \dfrac{sL_f\omega_r^2}{s^2 + \omega_r^2} \end{cases}, \quad \omega_r = \sqrt{\frac{1}{L_f C_f}}. \tag{2}$$

From Fig. 2(b), the open-loop transfer function $T_o(s)$ can be derived as

$$T_o(s) = G_c(s)G_d(s)G_{vc}(s). \tag{3}$$

Then the phase and magnitude of $T_o(s)$ can be calculated as (4).

$$\begin{cases} \angle T_o(j\omega) = \begin{cases} -1.5\omega T_s, & \omega_o << \omega < \omega_r \\ -\pi - 1.5\omega T_s, & \omega > \omega_r \end{cases} \\ \left|T_o(j\omega)\right| = \dfrac{k_p\omega_r^2}{\left|\omega_r^2 - \omega^2\right|}, \quad \omega >> \omega_o \end{cases}. \tag{4}$$

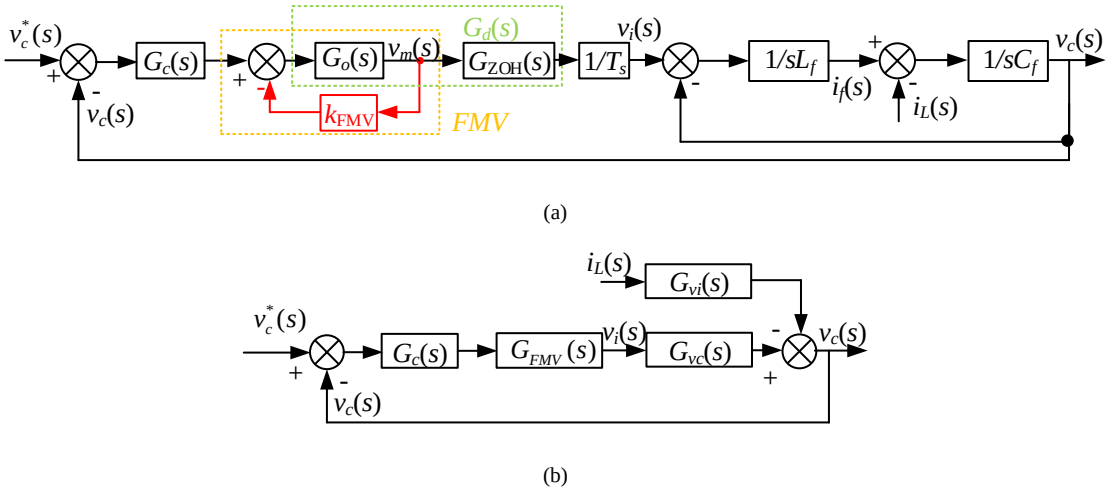


(a)




(b)

Fig. 4. Single-loop voltage control diagram with FMV in the continuous *s*-domain. (a) Block diagram. (b) Equivalent diagram.

Generally, the Nyquist stability criterion can be used to analyze the system stability by calculating the clockwise encirclements $N$ of (-1, $j$0) by the Nyquist curve of $T_o(s)$ and number of unstable open-loop poles $Z$ of $T_o(s)$. If $2N + Z = 0$, the system is stable, otherwise the system is unstable. The detailed analysis of the stability of conventional single-loop control system has been presented in [4] and [9]. And the stable region is derived as

$$-1.5\omega_r T_s < -\pi \Rightarrow \omega_r > \omega_s / 3. \tag{5}$$

Fig. 3 shows the Bode plots of $T_o(s)$ with a PR voltage controller. As seen, the -180° phase crossing happens always at the resonance frequency $\omega_r$ when $\omega_r < \omega_s/3$ due to the 180° phase jump, thus resulting in $N \neq 0$. Due to $Z = 0$, $2N + Z \neq 0$, which denotes instability. While when $\omega_r > \omega_s/3$, the -180° phase crossing is located at $\omega_s/3$, and the magnitude of $T_o(j\omega_s/3)$ could be less than 1 by setting a proper proportional gain $k_p$ to make $N$=0. Thus $2N + Z = 0$, the system can be stable.

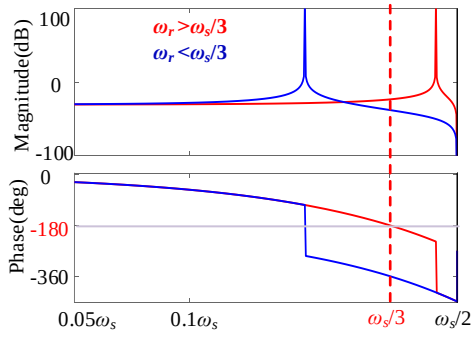


Fig. 3. Bode plots of open-loop transfer function $T_o(s)$ with a PR controller.

From (5) and Fig. 3, the resonant frequency $\omega_r$ should be designed to be high enough to ensure system stability. In this case, filter capacitance should be designed with a small values which makes the system sensitive to load disturbances and poses weaken attenuation ability against high frequency switching harmonics. Moreover, for the asymmetric regular sampling where $\omega_r$ should be less than $\omega_s/4$, it is difficult to achieve the stability design [8].

## III. Proposed Feedback of Modulation Voltage Control

### A. Feedback of Modulation Voltage Control

From previous analysis, $\omega_s/3$ can be regarded as a critical frequency caused by the phase lag for the conventional single-loop control. Stability of the system with resonant frequency higher than $\omega_s/3$ is totally different from that with resonant frequency smaller than $\omega_s/3$.

Therefore, if this critical frequency can be shifted to a smaller value without changing sampling frequency, then stability requirement of the system with a small resonant frequency could be satisfied.

This paper proposes a Feedback of Modulation Voltage (FMV) control method, the control diagram is shown in Fig.4. In Fig.4 (a), $v_m(s)$ represents the modulation voltage which is fed back to the control system with proportional gain $k_{FMV}$. $G_d(s)$ is divided into an unitary sampling period computational delay $G_o(s)$ and equivalent 0.5 sampling period delay $G_{ZOH}(s)$ for Pulse Width Modulation (PWM), expressed as

$$\begin{cases} G_o(s) = e^{-sT_s} \\ G_{ZOH}(s) = (1 - e^{-sT_s}) / s \end{cases}. \tag{6}$$

Fig.4 (b) shows the equivalent form of fig. 4(a). In the figure, $G_{FMV}(s)$ presents the total equivalent digital delay of the control system with FMV method, expressed as

$$\begin{aligned} G_{FMV}(s) &= \frac{1 - e^{-sT_s}}{sT_s} \frac{e^{-sT_s}}{1 + k_{FMV} e^{-sT_s}} \\ &= \frac{G_d(s)}{1 + k_{FMV} e^{-sT_s}} \end{aligned}. \tag{7}$$

According to (7), the phase of open-loop transfer function $T_{oM}(s)$ with FMV method can be calculated as (8).

$$\angle T_{oM}(j\omega) = \begin{cases} -1.5\omega T_s + \arctan\left(\dfrac{k_{\mathrm{FMV}}\sin(\omega T_s)}{1+k_{\mathrm{FMV}}\cos(\omega T_s)}\right) \\ \omega_o << \omega < \omega_r \\ -\pi - 1.5\omega T_s + \arctan\left(\dfrac{k_{\mathrm{FMV}}\sin(\omega T_s)}{1+k_{\mathrm{FMV}}\cos(\omega T_s)}\right) \\ \omega > \omega_r \end{cases} . \quad (8)$$

When $k_{\mathrm{FMV}} = 0$, (7) is equal to (2) while (8) is equal to (4), which represents for the conventional method. Therefore, conventional single loop method could be regarded as a special FMV method with $k_{\mathrm{FMV}} = 0$. Moreover, to ensure no unstable open-loop poles, constraints for $k_{\mathrm{FMV}}$ are derived as (9) with Routh criterion [6].

$$-1 < k_{FMV} < 1 . \quad (9)$$

According to (8) and (9), $k_{\mathrm{FMV}}$ can be either a positive or negative value, which leads to different frequency-phase characteristics of $T_{oM}(s)$. Therefore, it's necessary to investigate the system stability with different values of $k_{\mathrm{FMV}}$.

### B. *Stability with Negative $k_{\mathrm{FMV}}$*

When a negative $k_{\mathrm{FMV}}$ is applied to the control system, to ensure that the phase of $T_{oM}(s)$ at resonant frequency $\omega_r$ should not be equal to -180°, the constraint can be derived as

$$-1.5\omega_r T_s < -\pi + \arctan\left(\frac{|k_{\mathrm{FMV}}|\sin(\omega_r T_s)}{1+k_{\mathrm{FMV}}\cos(\omega_r T_s)}\right)$$
$$\Downarrow \quad . \quad (10)$$
$$\omega_r > \frac{\omega_s}{3} - 2\arctan\left(\frac{|k_{\mathrm{FMV}}|\sin(\omega_r T_s)}{1+k_{\mathrm{FMV}}\cos(\omega_r T_s)}\right)/(3T_s) = \omega_{rn}$$

From (10), resonant frequency $\omega_r$ should be higher than $\omega_{rn}$ to ensure system stability. Fig. 5 shows the Bode plots of $T_{oM}(s)$ with $k_{\mathrm{FMV}} = -0.9$, in this case $\omega_{rn}$ is derived as $0.259\omega_s$. As seen in Fig. 5(a), when $\omega_r < \omega_{rn}$ due to the 180° phase drop, thus resulting in $N \neq 0$. While when $\omega_r > \omega_{rn}$, the -180° phase crossing is located at $\omega_{rn}$, and the magnitude of $T_o(j\omega_{rn})$ could be less than 1 by setting a proper magnitude of $k_p$, thus $N=0$.

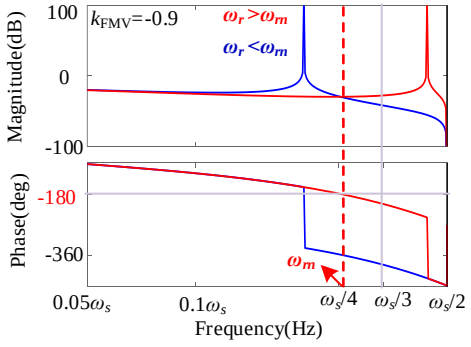


Fig. 5. Bode plots of open-loop transfer function $T_{oM}(s)$ with a negative $k_{\mathrm{FMV}}$.

Therefore, $\omega_{rn}$ can be regarded as the critical frequency for FMV method with a negative $k_{\mathrm{FMV}}$. It can be also found that $\omega_{rn} < \omega_s/3$, which means the critical frequency of the conventional method will be shifted to the left side with FMV method. As a result, the stability region of the system would be widened. Moreover, when $k_{\mathrm{FMV}}$ is selected to be close to -1, then $\omega_{rn}$ could be approximately derived as $\omega_s/4$. Compared to the conventional method, proposed FMV method with a negative $k_{\mathrm{FMV}}$ can widen the stable region from ($\omega_s/3$, $\omega_s/2$) to ($\omega_s/4$, $\omega_s/2$)

### C. *System Stability with Positive $k_{\mathrm{FMV}}$ and Negative $k_p$*

When a positive $k_{\mathrm{FMV}}$ is applied to the control system, to ensure that the phase of $T_{oM}(s)$ at resonant frequency $\omega_r$ should not be equal to -180°, the constraint can be derived as

$$-1.5\omega_r T_s < -\pi - \arctan\left(\frac{|k_{\mathrm{FMV}}|\sin(\omega_r T_s)}{1+k_{\mathrm{FMV}}\cos(\omega_r T_s)}\right)$$
$$\Downarrow \quad . \quad (11)$$
$$\omega_r > \frac{\omega_s}{3} + 2\arctan\left(\frac{|k_{\mathrm{FMV}}|\sin(\omega_r T_s)}{1+k_{\mathrm{FMV}}\cos(\omega_r T_s)}\right)/(3T_s) = \omega_{rp}$$

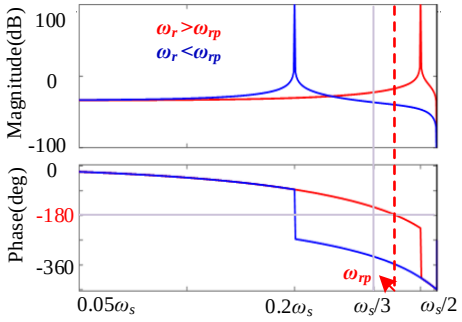


(a)

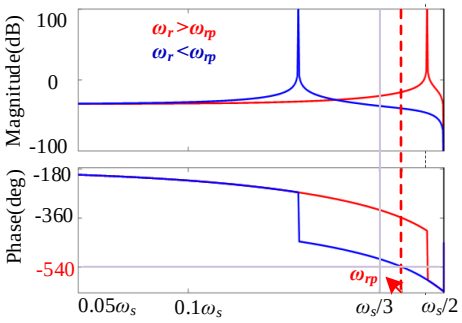


(b)

Fig. 6. Bode plots of open-loop transfer function $T_{oM}(s)$ with a positive $k_{\mathrm{FMV}}$. (a)$k_p > 0$. (b) $k_p < 0$.

Fig. 6(a) shows the Bode plots of $T_{oM}(s)$ with a positive $k_{\mathrm{FMV}}$. As seen in Fig. 6(a), when $\omega_r < \omega_{rp}$ due to the 180° phase drop, thus resulting in $N \neq 0$. While when $\omega_r > \omega_{rp}$, the -180° phase crossing is located at $\omega_{rp}$, and the magnitude of $T_{oM}(j\omega_{rp})$ could be less than 1 by setting a proper magnitude of $k_p$, thus $N=0$.

Therefore, $\omega_{rp}$ can be regarded as the critical frequency for FMV method with positive $k_{FMV}$. As opposite to the case with negative $k_{FMV}$, critical frequency will be shifted to right side of $\omega_s/3$. In previous analysis, proportional gain $k_p$ of $G_c(s)$ is generally designed to be a positive value. In this case, FMV method with a positive $k_{FMV}$ narrows the stable region from ($\omega_s/3$, $\omega_s/2$) to ($\omega_{rp}$, $\omega_s/2$), which lead to a worse stability characteristic.To widen the stable region, a negative $k_p$ is adopted in this section, which will provide -180° phase lag for the system. In this scenario, (8) is rewritten as (12).

$$\angle T_{oM}(j\omega) = \begin{cases} -\pi - 1.5\omega T_s + \arctan\left(\dfrac{k_{FMV}\sin(\omega T_s)}{1+k_{FMV}\cos(\omega T_s)}\right) \\ \omega_o << \omega < \omega_r \\ -2\pi - 1.5\omega T_s + \arctan\left(\dfrac{k_{FMV}\sin(\omega T_s)}{1+k_{FMV}\cos(\omega T_s)}\right) \\ \omega > \omega_r \end{cases} . \quad (12)$$

TABLE I
STABLE REGION

| | Stable region | |
|---|---|---|
| | $k_p > 0$ | $k_p < 0$ |
| $k_{FMV} > 0$ | ($\omega_s/3$, $\omega_s/2$) | **(0, $\omega_s/2$)** |
| $k_{FMV} = 0$ (Conventional method) | ($\omega_s/3$, $\omega_s/2$) | (0, $\omega_s/3$) |
| $k_{FMV} < 0$ | ($\omega_s/4$, $\omega_s/2$) | (0, $\omega_s/3$) |

As seen, with the increase of frequency, the phase of $T_{oM}(s)$ will decrease with the begin of -180°. Therefore, crossing at -540° rather than -180° should be taken into consideration. To ensure that the phase of $T_{oM}(s)$ at resonant frequency $\omega_r$ should not be equal to -540°(-3π), the constraint can be derived as

$$-1.5\omega_r T_s > -\pi - \arctan\left(\frac{|k_{FMV}|\sin(\omega_r T_s)}{1+k_{FMV}\cos(\omega_r T_s)}\right)$$
$$\Downarrow \quad . \quad (13)$$
$$\omega_r < \frac{\omega_s}{3} + 2\arctan\left(\frac{|k_{FMV}|\sin(\omega_r T_s)}{1+k_{FMV}\cos(\omega_r T_s)}\right)/(3T_s) = \omega_{rp}$$

Fig. 6(b) shows the Bode plots of $T_{oM}(s)$ with a positive $k_{FMV}$ and negative $k_p$. As seen, when $\omega_r < \omega_{rp}$, the -540° phase crossing is located at $\omega_{rp}$, and the magnitude of $T_{oM}(j\omega_{rp})$ could be less than 1 by setting a proper proportional gain $k_p$, thus $N = 0$. When $\omega_r > \omega_{rp}$ due to the 180° phase drop, the -540° phase crossing is located at $\omega_r$, thus resulting in $N \neq 0$. Therefore, the stable region is (0, $\omega_{rp}$). Moreover, when $k_{FMV}$ is selected to be close to 1, then $\omega_{rp}$ could be approximately derived as $\omega_s/2$. On the basis of analysis above, the maximum stable regions of the conventional method and proposed method are concluded in Table I. The derivation of stable region of conventional method with $k_p < 0$ is neglected since the analysis method is similar. As seen, Compared to the conventional method, the proposed FMV method with a positive $k_{FMV}$ and negative $k_p$ can reach maximum stable

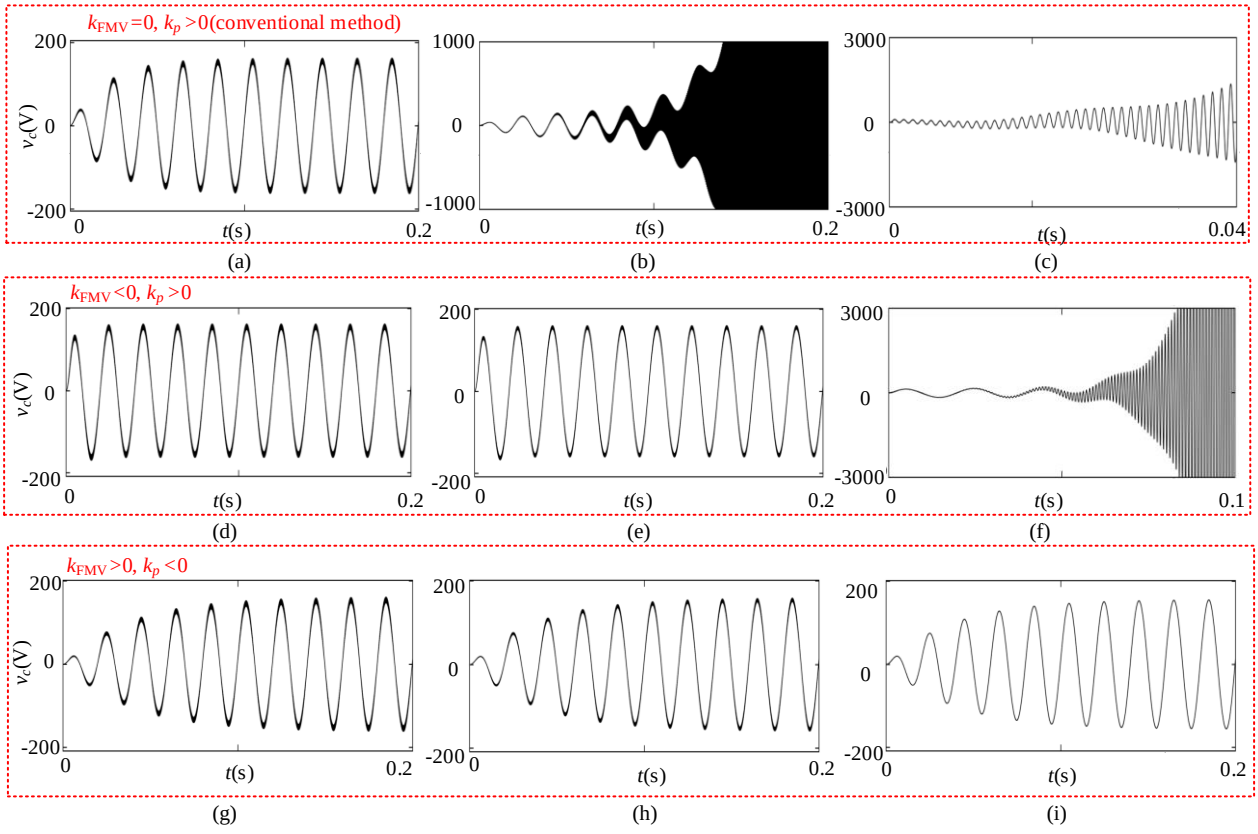


Fig. 7. Simulation results of the conventional single-loop method and the FMV method. (a)(d)(g) for Case I, (b)(e)(h) for Case II, (c)(f)(i) for Case III.

region by (0, $\omega_s$/2).

## IV. Simulation Results

In this section, stability performance of the conventional and FMV control design method is evaluated in the MATLAB/Simulink. The key system parameters are given in Table II.

TABLE II
SYSTEM PARAMETERS

| Description | Symbol | Value |
|---|---|---|
| Capacitor voltage | $v_c$ | 110 V(RMS) |
| DC voltage | $U_{dc}$ | 400 V |
| Fundamental frequency | $f_o$ | 50 Hz |
| Sampling frequency | $f_s$ | 10 kHz |
| Switching frequency | $f_{sw}$ | 5 kHz |
| LC inductance | $L_f$ | 1mH |
| LC capacitance | $C_f$ | 2/3/20 μF |
| Resonant freqeucny | $f_r$ | 3.56/2.90/1.12 kHz |
| Proportional gain | $k_p$ | 0.03/-0.03 |
| Resonant gain | $k_r$ | 100 |
| FMV gain | $k_{FMV}$ | 0.9/-0.9 |

In Table II, three different capacitors are simulated to present different resonance cases, i.e. Case I: resonant frequency is 3.56kHz; Case II: resonant frequency is 2.9kHz; Case III: resonant frequency is 1.12kHz. PR controller parameters of these cases are the same. Moreover, loads are no added in the system to consider the worst damping situation.

According to the above analysis, for the conventional method, the system can only be stable in Case I due to $f_r > f_s$ /3. For the FMV method with $k_{FMV}$ = -0.9 and $k_p$ = 0.03 the system be stable in both Case I and Case II due to 3.56 kHz >2.9 kHz >2.59 kHz (2.59 kHz is the critical frequency of FMV method with $k_{FMV}$=-0.9). For the FMV method with $k_{FMV}$ = 0.9 and $k_p$ = -0.03 ($k_p$ is designed to ensure that the magnitude of the open-loop transfer function should be less than 0dB at -180 degree crossing), the system can be stable in all cases. In this section, stability characteristics of above three methods in different cases are simulated.

Simulations results are shown in Fig. 7. For figures (a)-(c), the control system with the conventional method are simulated. For figures (d)-(f), the control system with the FMV method where $k_{FMV}$ <0 and $k_p$ >0 are simulated. For figures (g)-(i), the control system with the FMV method where $k_{FMV}$ >0 and $k_p$ <0 are simulated. In Case I, the system can be stable with both three methods, as show in Fig. 7(a), Fig. 7(d) and Fig. 7(g). When resonant frequency $f_r$ decreases to 2.9kHz, i.e. in Case II, the capacitor voltage of the control system with the conventional method starts to diverge, which denotes instability, seen in Fig. 7(b). Therefore, by modifying the value of $k_{FMV}$, the critical frequency will be shifted to the left of its original value, which enable a LC filter with smaller resonant frequency to be implemented in the converter. Moreover, when the resonant frequency is lower than $f_s$ /4, i.e. in Case III, the system can only be stable with FMV method where $k_{FMV}$ >0 and $k_p$ <0, seen in Fig. 7(i). The simulations results fit well with the above analysis, which proves the correctness of the proposed method.

## V. Conclusion

This paper proposes a feedback of modulation voltage control method based on conventional single-loop voltage control for low *LC*-resonant-frequency VSIs. By feeding back the modulation voltage with an unit delay to the control system through a negative or a positive proportional gain $k_{FMV}$, the critical frequency will be shifted to the left or shifted to the right. It is found that with a negative $k_p$ and positive $k_{FMV}$, the stable region of the system with FMV method can be extended to (0, $f_s$/2) at most, which significantly enhance the stability of the single-loop control VSIs system as well as increase the variability of resonant frequency, which helps in the design of the LC filter. However, this method leads to poor dynamic performance which can be solved with enhanced voltage control proposed in literature. Simulation results are finally provided to validate the correctness of the proposed method.


## Acknowledgement

The research leading to these results was supported by Wingrid Project with funding from the European Union's Horizon 2020 research and innovation programme under the Marie Sklodowska-Curie grant agreement No 861398, and Interreg Deutschland-Danmark with funds from the European Regional Development Fund via the PE-Region Platform project (ref. 098-1.1-18).


## Reference


[1] X. F. Wang, J. M. Guerrero, Z. Chen, and F. Blaabjerg, "Distributed energy resources in grid interactive AC microgrids," in *Proc. PEDG*, Heifei, China, 2010, pp. 806–812.

[2] Z. Li, Y. Li, P. Wang, H. Zhu, C. Liu, and F. Gao, "Single-loop digital control of high-power 400-Hz ground power unit for airplanes," *IEEE Trans. Ind. Electron.*, vol. 57, no. 2, pp. 532–543, Feb. 2010.

[3] M. J. Ryan, W. E. Brumsickle, and R. D. Lorenz, "Control topology options for single-phase UPS inverters," *IEEE Trans. Ind. Appl.*, vol. 33, no. 2, pp. 493–501, Mar./Apr. 1997.

[4] X. Wang, P. Loh, and F. Blaabjerg, "Stability Analysis and Controller Synthesis for Single-Loop Voltage-Controlled VSIs," *IEEE Trans. Power Electron.*, vol. 32, no. 9, pp. 7394-7404, Sep. 2017.

[5] W. Wu, Y. He, T. Tang, and F. Blaabjerg, "A New Design Method for the Passive Damped LCL and LLCL Filter-Based Single-Phase Grid-Tied Inverter," *IEEE Trans. Ind. Electron.*, vol. 60, no. 10, pp. 4339-4350, Oct. 2013.

[6] D. Pan, X. Ruan, C. Bao, W. Li and X. Wang, "Optimized Controller Design for LCL-Type Grid-Connected Inverter to Achieve High Robustness Against Grid-Impedance Variation," in *IEEE Transactions on Industrial Electronics*, vol. 62, no. 3, pp. 1537-1547, March 2015.

[7] U. B. Jensen, F. Blaabjerg, and J. K. Pedersen, "A new control method for400-Hz ground power units for airplanes," *IEEE Trans. Ind. Appl.*, vol. 36, no. 1, pp. 180–187, Jan./Feb. 2000.

[8] Y. Geng, Y. Yun, R. Chen, K. Wang, H. Bai, and X. Wu, "Parameters design and optimization for *LC*-type off-grid inverters with inductor-current feedback active damping," *IEEE Trans. Power Electron.*, vol. 33, no. 1, pp. 703–715, Jan. 2018.

[9] X. Li, P. Lin, Y. Tang, and K. Wang, "Stability Design of Single-Loop Voltage Control With Enhanced Dynamic for Voltage-Source Converters With a Low LC-Resonant-Frequency," *IEEE Trans. Power Electron.*, vol. 33, no. 11, pp. 9937-9951, Nov. 2018

[10] R. Zhu, M. Liserre, M. Langwasser and C. Kumar, "Operation and Control of the Smart Transformer in Meshed and Hybrid Grids: Choosing the Appropriate Smart Transformer Control and Operation Scheme," *IEEE Industrial Electronics Magazine*, vol.15, no. 1, pp. 43-57, March 2021.